Heat generation by spin-polarized current in a quantum dot connected to spin battery and ferromagnetic lead*

Bai Xu-Fang(白絮芳)[a], Sun Lian-Liang(孙连亮)[b], and Chi Feng(迟 锋)[c,d,†]

[a] College of Physics and Electronic Information, Inner Mongolia National University, Tongliao 028043, China
[b] College of Science, North China University of Technology, Beijing 100041, China
[c] School of Physical Science and Technology, Inner Mongolia University, Huhehaote 010023, China
[d] College of Engineering, Bohai University, Jinzhou 121013, China

(Received 24 October 2014; revised manuscript received 5 December 2014; published online 27 March 2015)

We study theoretically the heat originated from electron–phonon coupling in a spintronic device composed of a semiconductor quantum dot attached to one spin battery and one ferromagnetic lead. It is found that the phenomenon of the negative differential of the heat current, which has previously been predicted in the charge-based device, disappears due to the Pauli exclusion principle resulted from the presence of the spin battery. Under some conditions, huge heat in the heat generation induced by resonant phonon emitting processes also disappears in this spin-based device. Furthermore, we find that the ferromagnetism of the lead can be used to effectively adjust the magnitude of the heat current in different dot level ranges. The proposed system is realizable by current technology and may be useful in designing high-efficiency spintronic components.

Keywords: quantum dot, heat generation, spin battery, ferromagnetic lead

PACS: 73.21.La, 72.15.Jf, 73.50.Lw **DOI:** 10.1088/1674-1056/24/5/057302

1. Introduction

Continuous miniaturization of integrated circuits makes the problem of local heating generated by electric current more and more serious. This is because the amount of heat becomes huge as millions of submicro- and nano-scale components are assembled on a mainstream chip whose area is on the order of a square centimeter or smaller. If the heat is not removed or suppressed effectively, the temperature will rise so high it will break down the device's functionality. On the other hand, the huge local heating will unavoidably raise the device's energy consumption and shorten its work life. Consequently, understanding how the heat is generated and transported in miniaturized structures is crucial for both system's stability and designing energy conservation electric devices.[1] Many recent experimental works have been devoted to the detection of local heating in nanostructures,[2–6] and some effective ways of controlling heat dissipation were suggested.[7–9] From a microscopic point of view, the most important causes of heat dissipation are the inelastic electron–electron (e–e) and electron–phonon (e–p) collisions.[10–14] Strong e–p interaction in some low-dimensional systems has been observed through phonon-assisted tunnelling processes in recent experiments.[15–18] Previous works have shown that although having essentially the same cause of heat, some familiar laws of heat generation applicable in macroscopic systems, for example the Joule law, may not be valid in mesoscopic and nanoscale structures. Quantized energy carried by phonons has been predicted and further studied in various systems.[2,7,8,14] Theoretically, heat generation by electric current in mesoscopic devices has also been studied within the nonequilibrium Keldysh Green's function technique,[10,12] and some particular new quantum phenomena have been predicted.[10,12,19–32] Potential applications such as the nano-refrigerator[30] or heat rectifier[31] were recently suggested.

Very recently, interaction between electron spin and thermodynamics has aroused new interest in both spin caloritronics[33] and spintronics[34] due to the experimental breakthrough by Uchida *et al.*[35] They observed the spin Seebeck effect in semiconductor ferromagnets with temperature gradients across them. This effect refers to the generation of spin bias by temperature gradient in the absence of charge current, and is a spin analog of the usual Seebeck effect. Subsequently, Le Breton *et al.* observed a Seebeck spin current originated from the energy derivative of the tunnel spin polarization in a ferromagnet-oxide-silicon tunnel junction.[36] They showed that the heat current in spintronic devices sensitively depends on the different thermal electron distribution in the electron reservoirs and the energy variation of the tunneling spin polarization. This is completely different from the case in charge-based systems.

To investigate the effect of energy-dependence of the tunnelling spin polarization on heat generation, we propose a system composed of a semiconductor quantum dot (QD) coupled simultaneously to a spin battery and a ferromagnetic lead

*Project supported by the National Natural Science Foundation of China (Grant No. 61274101).
†Corresponding author. E-mail: chifeng@bhu.edu.cn
© 2015 Chinese Physical Society and IOP Publishing Ltd

in the present paper (see Fig. 1). The QD or QD molecular are man-made zero-dimensional structures in solid, in which electrons are confined in all three directions and exhibit fully quantized energy levels.[37] As compared to some previously studied heterostructures,[38–41] parameters of the QD structure, such as the electron number on the dot, dot level, and coupling strength between the dot and electron reservoirs, can be precisely adjusted by external gate voltages. Various QD-based nano-systems have been fabricated and successfully used in functional devices due to their many particular electric and photoelectric properties.[37] Semiconductor QD has also become one of the most important objects in spintronics,[34] whose central theme is the active manipulation of spin degrees of freedom in solid-state systems. Semiconductor spacers of InAs QD with a controllable size and energy spectrum has been inserted in between nickel or cobalt leads.[42] In such a device, the spin polarization of the current injected from the ferromagnetic leads can be effectively tuned by a gate nearby the QD, and opens new possible applications. Until now, many effective methods have been developed to generate and control spin-polarized current in semiconductor spintronics, including electrical,[34,43] optical[44,45] and even thermal techniques.[35,36,46] The current polarization can reach as high as 100% or even infinite. Among various schemes for generating and manipulating spin-polarized current, the spin battery or spin cell may be the most effective one. While a charge battery provides a bias voltage to drive the flow of electrons, a spin battery can provide spin-dependent chemical potentials to behave as the driving force for the flow of electron spin (see Fig. 1). Pure spin current driven out from the spin battery has recently been electrically generated in a micro-wide quantum wire defined by electrostatic gates on top of a GaAs/AlGaAs heterostructure.[47–49] Some theoretical proposals for spin battery[50,51] were also suggested. Our following results will show that the properties of the heat generation in the presence of the spin battery are quite different from those previously found in systems subjected to the usual charge bias. For example, the negative differential of the heat current disappears due to the Pauli exclusion principle as the spin-degenerate energy level cannot be simultaneously occupied by electrons of the same spin orientation. The ferromagnetism of the lead can be used to effectively tune the current's strength and the magnitude of the heat current in different dot level's regimes.

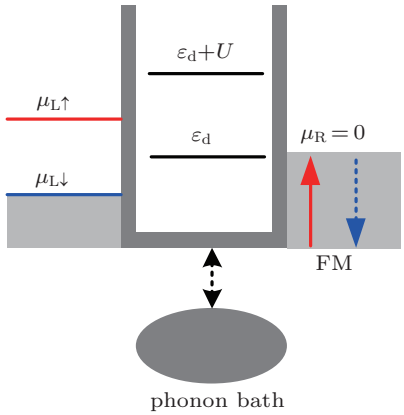


Fig. 1. (color online) Schematic plot of a quantum dot coupled to the left spin battery and the right ferromagnetic lead. The spin battery induces spin-dependent chemical potentials in the left lead. The heat results from the electron–phonon interaction, through which the energy associated with the spin-polarized current passing through the dot is transferred to the phonon bath in the form of heat.

2. Model and method

We consider a single-level molecular QD connected to the left spin battery and the right ferromagnetic lead. There is a gate electrode contacted to the dot to adjust the dot energy level. The electrons on the dot are coupled to a single-phonon mode. The total Hamiltonian of the system can be written as[10,12,19] $H = H_{\rm leads} + H_{\rm ph} + H_{\rm dot} + H_{\rm T}$, where $H_{\rm leads} = \sum_{k,\sigma,\beta\in{\rm L,R}} \varepsilon_{k\beta\sigma} c^{\dagger}_{k\beta\sigma} c_{k\beta\sigma}$ is the Hamiltonian for electrons in the left (L) and right (R) leads, and $c^{\dagger}_{k\beta\sigma}$ ($c_{k\beta\sigma}$) is the conduction electron creation (annihilation) operator with wave vector k, spin-dependent electron energy $\varepsilon_{k\beta\sigma}$, and spin σ. The second term stands for the single-phonon mode $H_{\rm ph} = \omega_q a^{\dagger} a$, where $a^{\dagger}(a)$ is the creation (annihilation) operator of a phonon having frequency ω_q. The third term is the electron Hamiltonian on the QD[10,12,19,52]

$$H_{\rm D} = \sum_{\sigma} [\varepsilon_0 + \lambda(a^{\dagger} + a)] d^{\dagger}_{\sigma} d_{\sigma} + U_0 d^{\dagger}_{\uparrow} d_{\uparrow} d^{\dagger}_{\downarrow} d_{\downarrow}, \qquad (1)$$

where $d^{\dagger}_{\sigma}$ (d_{σ}) creates (annihilates) an electron with energy ε_0 and intradot Coulomb interaction U_0. The quantity λ is the coupling constant between the dot electron and located phonon mode. The last term $H_{\rm T} = \sum_{k,\beta,\sigma} (V_{k\beta\sigma} c^{\dagger}_{k\beta\sigma} d_{\sigma} + {\rm H.c})$ describes the conduction electron hopping between the QD and the leads with $V_{k\beta\sigma}$ being the spin-dependent tunnelling matrix element. In our considered system, only $V_{k{\rm R}\sigma}$ really depends on spin due to the existence of the ferromagnetic electrode. We add a spin index for $V_{k{\rm L}\sigma}$ for the sake of uniformity.

The spin-dependent electric current flowing through the structure can be calculated with the help of the Keldysh nonequilibrium Green's function formalism, and its standard form is obtained as[53–55]

$$J_{\sigma} = -\frac{e}{h} \int \frac{{\rm d}\omega}{2\pi} [f_{{\rm L}\sigma}(\omega) - f_{{\rm R}\sigma}(\omega)] \frac{\Gamma_{{\rm L}\sigma}\Gamma_{{\rm R}\sigma}}{\Gamma_{{\rm L}\sigma} + \Gamma_{{\rm R}\sigma}} {\rm Im} G^{\rm r}_{\sigma}(\omega), \quad (2)$$

where the dot single-electron Green's functions $G^{\rm r,a,<,>}_{\sigma}(\omega)$ are the Fourier transforms of $G^{\rm r,a,<,>}_{\sigma}(t)$, i.e., the retarded (advanced) one $G^{\rm r(a)}_{\sigma}(t) = \mp {\rm i}\theta(\mp t)\langle\{d_{\sigma}(t), d^{\dagger}_{\sigma}(0)\}\rangle$, the lesser Green's function $G^{<}_{\sigma}(t) = {\rm i}\langle d^{\dagger}_{\sigma}(0) d_{\sigma}(t)\rangle$, and the greater Green's function $G^{>}_{\sigma}(t) = -{\rm i}\langle d^{\dagger}_{\sigma}(t) d_{\sigma}(0)\rangle$.[10] The Fermi distribution function is $f_{{\rm L(R)}\sigma}(\omega) = 1/\{\exp[\omega - \mu_{{\rm L(R)}\sigma}]/k_{\rm B}T_{\rm e} + 1\}$,[49–52] where $\mu_{\beta\sigma}$ and $T_{\rm e}$ are the spin-dependent chemical

potential in lead β and the temperature of the electrons, respectively. Here, similar to the tunnelling matrix element, only the chemical potentials of the left lead depend on spin, but we add a spin index for $\mu_{\mathrm{R}\sigma} = \mu_{\mathrm{R}}$. The line-width function in Eq. (2) is given by $\Gamma_{\beta\sigma} = 2\pi|V_{k\beta\sigma}|^2\rho_{\beta\sigma}$ and $\rho_{\beta\sigma}$ being the spin-dependent local density of states in lead β. In the real case, the ferromagnetism on the lead results from the spin-dependent band structure or density of states. Here, as a equivalent choice, we assume square bands of both spin-up and spin-down electrons (wide band approximation) and assume spin-dependent tunneling matrix $V_{k\beta\sigma}$. The spin-dependent line-width function of the right lead $\Gamma_{\mathrm{R}\sigma}$ is defined in terms of a spin-polarization parameter $p = (\Gamma_{\mathrm{R}\uparrow} - \Gamma_{\mathrm{R}\downarrow})/(\Gamma_{\mathrm{R}\uparrow} + \Gamma_{\mathrm{R}\downarrow})$, or $\Gamma_{\mathrm{R}\sigma} = \Gamma_{\mathrm{R}0}(1 + \sigma p)$.[54]

Due to the existence of the electron–phonon interaction, the calculation of the Green's functions is quite difficult. Following previous work, we make a canonical transformation to eliminate the electron–phonon coupling terms, i.e.,[10,12,53–55] $\tilde{H} = XHX^{\dagger}$ with $X = \exp[(\lambda/\omega_{\mathrm{q}})(a^{\dagger} - a)d^{\dagger}d]$. The transformed Hamiltonian reads

$$\begin{aligned}\tilde{H} = &\sum_{k,\beta\sigma} \varepsilon_{k\sigma\beta} c^{\dagger}_{k\beta\sigma} c_{k\beta\sigma} + \omega_{\mathrm{q}} a^{\dagger} a + \sum_{\sigma} \varepsilon_{\mathrm{d}} d^{\dagger}_{\sigma} d_{\sigma} + U d^{\dagger}_{\uparrow} d_{\uparrow} d^{\dagger}_{\downarrow} d_{\downarrow} \\ &+ \sum_{k,\alpha\sigma} (\tilde{V}_{k\beta\sigma} c^{\dagger}_{k\alpha\sigma} d_{\sigma} + \mathrm{H.c}), \end{aligned} \tag{3}$$

where the renormalized dot level and the intradot Coulomb interaction are respectively given by $\varepsilon_{\mathrm{d}} = \varepsilon_0 - g\omega_{\mathrm{q}}$ and $U = U_0 - 2g\omega_{\mathrm{q}}$ with $g = (\lambda/\omega_{\mathrm{q}})^2$. The tunnelling matrix element is also renormalized to $\tilde{V}_{k\alpha\sigma} = V_{k\alpha\sigma} X$, where the phonon operator $X = \exp[-g(a^{\dagger} - a)]$. Replacing X by its expectation value $\langle X\rangle = \exp[-g(N_{\mathrm{ph}} + 1/2)]$, the line-width function is renormalized to $\tilde{\Gamma}_{\beta\sigma} = \exp[-g(2N_{\mathrm{ph}} + 1)]\Gamma_{\beta\sigma}$, where $N_{\mathrm{ph}} = 1/[\exp(\omega_{\mathrm{q}}/k_{\mathrm{B}}T_{\mathrm{ph}}) - 1]$ being the phonon distribution function with T_{ph} the temperature of the phonon bath. In the above canonical transformation, the operators $a^{\dagger}a$ and $d^{\dagger}_{\sigma}d_{\sigma}$ remain unchanged, and then the heat flowing between the electrons and the phonons $Q(t) = \omega_{\mathrm{q}}\langle \mathrm{d}a^{\dagger}(t)a(t)/\mathrm{d}t\rangle$ can be calculated from the transformed Hamiltonian in Eq. (3). Without any time-dependent fields, the Fourier transform of $Q(t)$ can be obtained as[10,12,19]

$$\begin{aligned} Q = &\,\mathrm{Re}\sum_{\sigma} \omega_{\mathrm{q}} \lambda_{\mathrm{q}}^2 \int \frac{\mathrm{d}\omega}{2\pi} \{\tilde{G}^{<}_{\sigma}(\omega)\tilde{G}^{>}_{\sigma}(\bar{\omega}) \\ &- 2N_{\mathrm{ph}}[\tilde{G}^{>}_{\sigma}(\omega)\tilde{G}^{\mathrm{a}}_{\sigma}(\bar{\omega}) + \tilde{G}^{\mathrm{r}}_{\sigma}(\omega)\tilde{G}^{>}_{\sigma}(\bar{\omega})]\}, \end{aligned} \tag{4}$$

where $\bar{\omega} = \omega - \omega_{\mathrm{q}}$, and $\tilde{G}^{\mathrm{r,a},<,>}_{\sigma}(\omega)$ are the Fourier transforms of the usual single-particle Green's function $\tilde{G}^{\mathrm{r,a},<,>}_{\sigma}(t)$ defined in a similar way of $G^{\mathrm{r,a},<,>}_{\sigma}(t)$ based on the Hamiltonian (3). By employing the equation of motion technique, the retarded Green's function is obtained as[12]

$$\begin{aligned} \tilde{G}^{\mathrm{r}}_{\sigma}(\omega) = &\frac{1 - \langle n_{\bar{\sigma}}\rangle}{\omega - \varepsilon_{\mathrm{d}} + \mathrm{i}(\tilde{\Gamma}_{\mathrm{L}\sigma} + \tilde{\Gamma}_{\mathrm{R}\sigma})/2} \\ &+ \frac{\langle n_{\bar{\sigma}}\rangle}{\omega - \varepsilon_{\mathrm{d}} - U + \mathrm{i}(\tilde{\Gamma}_{\mathrm{L}\sigma} + \tilde{\Gamma}_{\mathrm{R}\sigma})/2}. \end{aligned} \tag{5}$$

Other Green's functions in Eq. (4) can be determined with the help of the retarded Green's function, i.e., $\tilde{G}^{\mathrm{a}}_{\sigma}(\omega) = [\tilde{G}^{\mathrm{r}}_{\sigma}(\omega)]^*$, $\tilde{G}^{<(>)}_{\sigma}(\omega) = \tilde{G}^{\mathrm{r}}_{\sigma}(\omega)\tilde{\Sigma}^{<(>)}_{\sigma}\tilde{G}^{\mathrm{a}}_{\sigma}(\omega)$, in which the lesser and greater self-energies are respectively given by $\tilde{\Sigma}^{<}_{\sigma} = \mathrm{i}[\tilde{\Gamma}_{\mathrm{L}\sigma} f_{\mathrm{L}\sigma}(\omega) + \tilde{\Gamma}_{\mathrm{R}\sigma} f_{\mathrm{R}\sigma}(\omega)]$, and $\tilde{\Sigma}^{>}_{\sigma} = -\mathrm{i}\{\tilde{\Gamma}_{\mathrm{L}\sigma}[1 - f_{\mathrm{L}\sigma}(\omega)] + \tilde{\Gamma}_{\mathrm{R}\sigma}[1 - f_{\mathrm{R}\sigma}(\omega)]\}$.[52,53] Next we need to calculate the electron Green's functions $G^{\mathrm{r,a},<,>}_{\sigma}(\omega)$, which have similar relationships as those between $\tilde{G}^{\mathrm{r,a},<,>}_{\sigma}(\omega)$, and then we need only the knowledge of $G^{\mathrm{r}}_{\sigma}(\omega)$. Based on the above canonical transformation between Eqs. (1) and (3), $G^{\mathrm{r}}_{\sigma}(\omega)$ is related to $\tilde{G}^{\mathrm{r}}_{\sigma}(\omega)$ by[53,54]

$$\begin{aligned} G^{\mathrm{r}}_{\sigma}(\omega) = &\sum_{n=-\infty}^{n=\infty} L_n \{\tilde{G}^{\mathrm{r}}_{\sigma}(\omega - n\omega_{\mathrm{q}}) \\ &+ \frac{1}{2}[\tilde{G}^{<}_{\sigma}(\omega - n\omega_{\mathrm{q}}) - \tilde{G}^{<}_{\sigma}(\omega + n\omega_{\mathrm{q}})]\}, \end{aligned} \tag{6}$$

where

$$L_n = \exp[-g(2N_{\mathrm{ph}} + 1)] \exp(n\omega_{\mathrm{q}}/2k_{\mathrm{B}}T) I_n[2g\sqrt{2N_{\mathrm{ph}}(N_{\mathrm{ph}} + 1)}],$$

with $I_n(x)$ the modified n-th Bessel function. The intradot occupation number now can be self-consistently calculated from the equation of

$$\langle n_{\sigma}\rangle = -\int \frac{\mathrm{d}\omega}{\pi} \frac{\Gamma_{\mathrm{L}\sigma} f_{\mathrm{L}\sigma}(\omega) + \Gamma_{\mathrm{R}\sigma} f_{\mathrm{R}\sigma}(\omega)}{\Gamma_{\mathrm{L}\sigma} + \Gamma_{\mathrm{R}\sigma}} \mathrm{Im} G^{\mathrm{r}}_{\sigma}(\omega). \tag{7}$$

3. Numerical results

In the following numerical investigations, we fix the chemical potential of the right ferromagnetic lead $\mu_{\mathrm{R}\uparrow} = \mu_{\mathrm{R}\downarrow} = \mu_{\mathrm{R}} = 0$ as the energy zero point, and choose the intradot e–e interaction $U = 1$ as the energy unit. Constants of $\hbar$ and k_{B} are all set to be 1. On assuming symmetric barriers, we have $\tilde{\Gamma}_{\mathrm{L}0} = \tilde{\Gamma}_{\mathrm{R}0} = \Gamma_0$. We also assume that the QD and the phonon bath are held at the same temperature, i.e., $T_{\mathrm{ph}} = T_{\mathrm{e}}$. The spin bias provided by the spin battery is related to the chemical potentials of the left lead via $V_{\mathrm{s}} = \mu_{\mathrm{L}\uparrow} = -\mu_{\mathrm{L}\downarrow}$, which is shown in Fig. 1. In the present paper we only consider the case of positive spin bias because the properties of the heat generation are independent of the current's direction. Figures 2(a) and 2(b) show the current and heat generation as functions of the spin bias when the dot is coupled to the left spin battery and right normal metal lead ($p = 0$). For the chosen parameters, the dot level locates between the left spin-up chemical potential and the right spin-independent chemical potential, i.e., $\mu_{\mathrm{L}\uparrow} > \varepsilon_{\mathrm{d}} > \mu_{\mathrm{R}}$. Consequently, only a spin-up electron can transport through the dot via ε_{d}. The spin-down current is zero as $\varepsilon_{\mathrm{d}} > \mu_{\mathrm{R}} > \mu_{\mathrm{L}\downarrow}$. It is shown in Fig. 2(a) that the current $J_{\uparrow}$ increases when the renormalized dot level ε_{d}

enters into the transport window of the spin bias, and then reaches a plateau. Unlike the condition of the system subjected to electric bias,[19] there is only one current plateau. It means that electrons cannot take the level of $\varepsilon_d + U$ to transport through the system. The reason is that the level ε_d in the transport window is partially occupied by spin-up electrons, and then $\varepsilon_d + U$ remains at empty due to the Pauli exclusion principle. With rasing temperature, the current's lineshape becomes smoother with qualitatively unchanged behaviors. There are also some phonon-induced sub-levels, at which the spin-polarized current increases due to the phonon-assisted tunneling processes.[10,19,53,54]

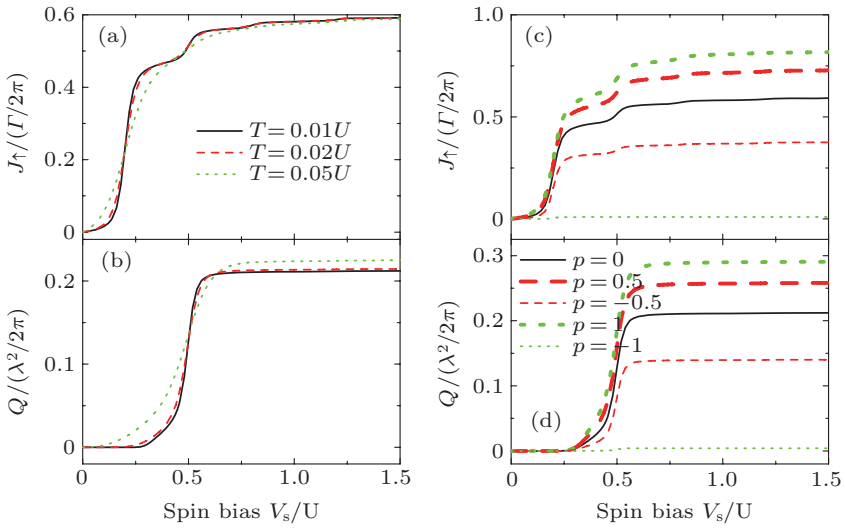


Fig. 2. (color online) Spin-up current and heat generation as functions of the spin bias at the left lead for different values of the temperature in panels (a) and (b), and different values of the spin polarization in the right lead in panels (c) and (d). Other parameters are $\omega_q = 0.3U$, $\lambda = 0.6\omega_q$, $\varepsilon_d = 0.2U$, and $\Gamma_0 = 0.01U$. The spin polarization of the right lead in panels (a) and (b) is zero, and the temperature in panels (c) and (d) is $T = 0.01U$.

As compared to Fig. 2(a), the heat generation in Fig. 2(b) has no direct relationship with respect to the spin-polarized current, indicating the breakdown of the Joule law for the heat generation applicable in bulk macroscopic systems. Similar to the case under electric bias,[10,19] the heat generation remains almost at zero for $V_s < \omega_q$ in the low temperature regime. The reason is that the phonon emitting process induced by electrons jumping between states of ω and $\omega - \omega_q$ needs to absorb enough energy from the external bias. There is also only one plateau in the heat generation whose rapid jump happens at $\varepsilon_d + \omega_q$, with a delay of ω_q with respect to the spin bias as compared to the electric current. Again, the curve of the heat generation becomes smoother with increasing temperature, and has no phonon-assisted sub-peak in the heat generation. We emphasize here that due to the Pauli exclusion principle mentioned above, the negative differential of the heat generation, which was predicted in a system subjected to charge bias,[19] disappears in the present structure. The reason is that this effect happens when the chemical potential of the source lead locates between $\varepsilon_d + U$ and $\varepsilon_d + U - \omega_q$, which are all empty here and the phonon absorbtion process can then not occur.

Figures 2(c) and 2(d) present $J_\uparrow$ and Q versus the spin bias for different values of spin-polarization of the right lead p. For comparison, the curves of $J_\uparrow$ and Q for $p = 0$ are also given. For $p > 0$, the strength of the line-width function of the right lead is enlarged, and then the magnitude of the spin-up current is enhanced accordingly. As $p = 1$, which corresponds to the case of a half-metallic right lead, the current's intensity reaches its maximum. For negative p, the magnitude of the current is decreased due to the reduction of the spin-up line-width function. Here the spin-down electron has no impact on the current and the heat because it cannot transport through the dot. The behavior of the heat generation in Fig. 2(d) resembles that of the current in Fig. 2(c).

Figure 3 shows the dependence of the current, heat generation, and electron occupation number on the dot level for different values of the spin bias. Both spin-up and spin-down currents in Fig. 3(a) are almost zero in the dot level range of $-U < \varepsilon_d < 0$ regardless of the value of the spin bias. This is because now a spin-up electron is injected from the left lead due to $\mu_{L\uparrow} > \varepsilon_d$, and it can hardly tunnel out of the dot to the right lead as $\mu_R > \varepsilon_d$. In this way a spin-up electron is blockaded on the dot and then spin-up current is nearly zero. Meanwhile, the spin-down energy level $\varepsilon_d + U$ is always kept out of its transport window ($\varepsilon_d + U > \mu_R, \mu_{L\downarrow}$), and is empty. In this dot level regime, since neither spin-up nor spin-down electrons can tunnel through the dot and then the heat generation in Fig. 3(b) is zero. The behavior of the occupation number is

illustrated in Fig. 3(c). When the dot level is in the range of $-(V_s+U)<\varepsilon_d<-U$, the spin-down energy level enters into its transport window resulting in finite $J_\downarrow$ and zero $J_\uparrow$. If the dot level is further lowered, both ε_d and ε_d+U are occupied by electrons of opposite directions (Fig. 3(c)), and then both spin-up and spin-down currents are zero as shown in Fig. 3(a). As a result, the heat generation in this dot level regime is zero. In the case of a higher dot level, i.e., $\varepsilon_d>V_s$, the dot is empty and both the currents and the heat generation are zero as discussed above. When the spin bias is slightly larger than ω_q, the curve $Q-\varepsilon_d$ has peaks respectively located at $\varepsilon_d=V_s/2\pm\omega_q/2$ and $\varepsilon_d=-U-V_s/2\pm\omega_q/2$.[10,19] Whereas the curve $J_{\uparrow(\downarrow)}-\varepsilon_d$ is quite flat, which shows again that the heat generation is not proportional to the current.

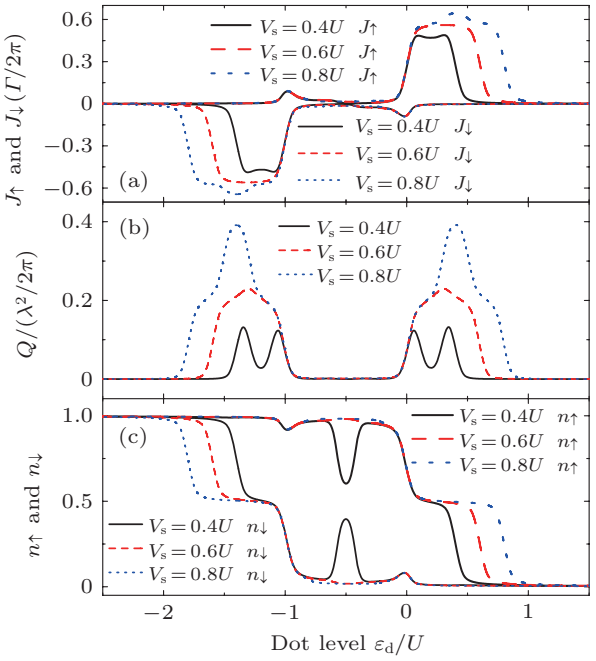


Fig. 3. (color online) (a) Spin-resolved currents, (b) heat generation, and (c) spin-resolved electron occupation numbers on the dot as functions of the dot level for indicated parameters. The temperature and the line-width function are all set to be $0.01U$, with $\omega_q=0.3U$, $\lambda=0.6\omega_q$, and $p=0$.

Figure 4 shows how the ferromagnetism on the right lead influences the quantities in Fig. 3. For $p=0$, spin-up and spin-down currents with opposite directions and equal strength emerge respectively in the dot level regimes of $0<\varepsilon_d<V_s$ and $-(V_s+U)<\varepsilon_d<-U$ as shown by the thick and thin solid lines in Fig. 4(a). The heat generation then develops two peaks at the centers of these two dot level regimes (solid line in Fig. 4(b)). Increasing the spin polarization from zero to a unit, the intensity of the spin-up (spin-down) current is enhanced (suppressed) for $0<\varepsilon_d<V_s$, and the intensity of the heat generation is adjusted accordingly. Decreasing the spin polarization from zero to a negative unit, a similar phenomenon occurs in the dot level regime of $-(V_s+U)<\varepsilon_d<-U$. We also find that the electron occupation number is changed by the ferromagnetism of the lead. For example when $p=1$, the spin-up line-width function increases and an electron of this spin component can transport through the dot easier in the dot level regime of $0<\varepsilon_d<V_s$. As a result of it, the spin-up electron number on the dot is decreased with enhanced heat generation. Finally, we argue that under the condition of $V_s<U$, the huge peak in the heat generation resulted from resonant phonon emitting when the renormalized intradot Coulomb interaction is equal to the phonon frequency ω_q, which has been predicted in a system with charge bias, cannot occur in the present device (not shown in the figure). The reason is that such an effect emerges when electrons are jumping from levels of ε_d and ε_d+U, which cannot be simultaneously occupied in the present system. The other previously found peak when the magnitude of the line-width function is near to the phonon energy quanta still exists, which is also not shown in the present paper.

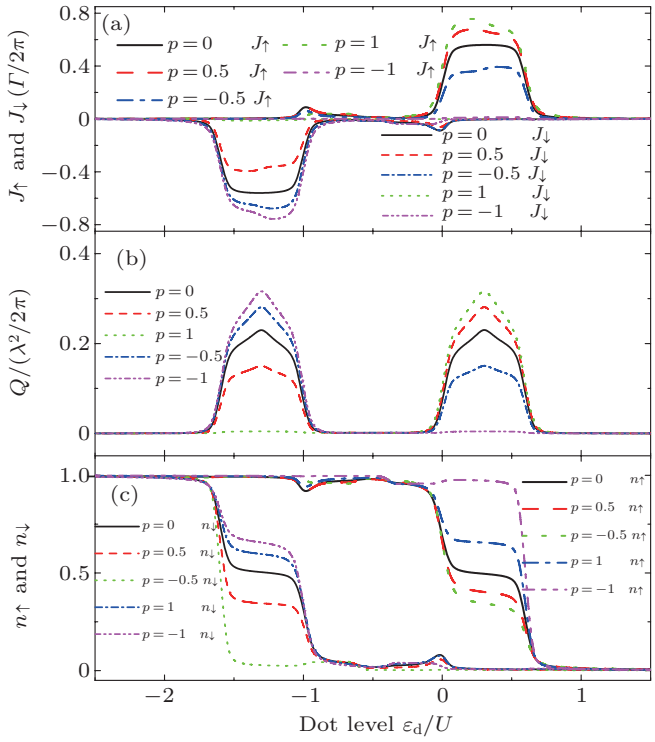


Fig. 4. (color online) (a) Spin-resolved currents, (b) heat generation, and (c) spin-resolved electron occupation numbers on the dot as functions of the dot level for $V_s=0.6U$. Other parameters are the same as in Fig. 3.

4. Conclusion

In conclusion, we have studied the properties of the heat generation in a QD coupled simultaneously to a spin battery and a ferromagnetic lead. We find that, inconsistent with a recent experimental work, the heat generation in this spintronic device is sensitive to the energy configuration of the spin-up and spin-down electrons. The introduction of the spin bias makes the properties of the heat generation quite different from those in a system subjected to charge bias. For example, both the negative differential of the heat generation and the

huge peak resulted from resonant phonon emitting disappear due to the Pauli exclusion principle. The ferromagnetism on the lead can be used to adjust the current intensity in different ranges of the dot level, and then the magnitude of the heat generation is controlled.

References

[1] Dubi Y and Di Ventra M 2011 *Rev. Mod. Phys.* **83** 131
[2] Schwab K, Henriksen E A, Worlock J M and Roules M L 2000 *Nature* **404** 974
[3] Balandin A 2011 *Nat. Mater.* **10** 569
[4] Huang Z, Xu B Q, Chen Y C, Di Ventra M and Tao N J 2006 *Nano Lett.* **6** 1240
[5] Huang Z, Chen F, D'Agosta R, Bennett P A, Di Ventra M and Tao N J 2007 *Nat. Nanotechnol.* **2** 698
[6] Oron-Carl M and Krupke R 2008 *Phys. Rev. Lett.* **100** 127401
[7] Rego L G C and Kirczenow G 1998 *Phys. Rev. Lett.* **81** 232
[8] Blencowe M P 1999 *Phys. Rev. B* **59** 4992
[9] Yamamoto T and Watanabe K 2006 *Phys. Rev. Lett.* **96** 255503
[10] Sun Q F and Xie X C 2007 *Phys. Rev. B* **75** 155306
[11] Lü J T and Wang J S 2007 *Phys. Rev. B* **76** 165418
[12] Wu B H and Cao J C 2009 *J. Phys.: Condens. Matter* **21** 245301
[13] Wang J S, Wang J and Lü J T 2008 *Eur. Phys. J. B* **62** 381
[14] Li N B, Ren J, Wang L, Zhang G, Hänggi P and Li B W 2012 *Rev. Mod. Phys.* **84** 1045
[15] Fujisawa T, Oosterkamp T H, van der Wiel W G, Broer B W, Aguado R, Tarucha S and Kouwenhoven L P 1998 *Science* **282** 932
[16] Park H, Park J, Lim A K L, Anderson E H, Alivisatos A P and McEuen P L 2000 *Nature* **407** 57
[17] LeRoy B J, Lemay S G, Kong J and Dekker C 2004 *Nature* **432** 371
[18] LeRoy B J, Kong J, Pahilwani V K, Dekker C and Lemay S G 2005 *Phys. Rev. B* **72** 075413
[19] Liu J, Song J T, Sun Q F and Xie X C 2009 *Phys. Rev. B* **79** 161309(R)
[20] Pei W, Xie X C and Sun Q F 2012 *J. Phys.: Condens. Matter* **24** 415302
[21] Pei W and Sun Q F 2012 *J. Appl. Phys.* **112** 124306
[22] Zhou L L 2011 *Chin. Phys. Lett.* **28** 128504
[23] Zhou L L, Li S S, Wei J N and Wang S Q 2011 *Phys. Rev. B* **83** 195303
[24] Zhou L L, Li S S and Zeng Z Y 2009 *Chin. Phys. Lett.* **26** 037304
[25] Deng Y X, Yan X H, Xiao Y and Tang N S 2010 *Phys. Lett. A* **374** 4375
[26] Wang Q, Xie H, Jiao H and Nie Y H 2013 *Europhys. Lett.* **101** 47008
[27] Chen Q and Zhang Y M 2010 *Commun. Theor. Phys.* **54** 171
[28] Chen Q and Deng Y H 2011 *Commun. Theor. Phys.* **56** 517
[29] Chen Q, Tang L M, Chen K Q and Zhao H K 2013 *J. Appl. Phys.* **114** 084301
[30] Chi F, Zheng J, Liu Y S and Guo Y 2012 *Appl. Phys. Lett.* **100** 233106
[31] Li B X, Zheng J and Chi F 2014 *Chin. Phys. Lett.* **31** 057302
[32] Guo Y, Sun L L and Chi F 2014 *Commun. Theor. Phys.* **62** 423
[33] Johnson M and Silsbee R H 1987 *Phys. Rev. B* **35** 4959
[34] Hanson R, Kouwenhoven L P, Petta J R, Tarucha S and Vandersypen L M K 2007 *Rev. Mod. Phys.* **79** 1217
[35] Uchida K, Takahashi S, Harii K, Ieda J, Koshibae W, Ando K, Maekawa S and Saitoh E 2008 *Nature* **455** 778
[36] Le Breton J C, Sharma S, Saito H, Yuasa S and Jansen R 2011 *Nature* **475** 82
[37] van der Wiel W G, De Franceschi S, Elzerman J M, Fujisawa T, Tarucha S and Kouwenhoven L P 2003 *Rev. Mod. Phys.* **75** 1
[38] Guo Y, Gu B L, Yu J Z, Zeng Z and Kawazoe Y 1998 *J. Appl. Phys.* **84** 918
[39] Guo Y, Wang H, Gu B L and Kawazoe Y 2000 *Phys. Rev. B* **61** 1728
[40] Guo Y, Qin J H, Chen X Y and Gu B L 2003 *Chin. Phys. Lett.* **20** 1124
[41] Guo Y, Shang C E and Chen X Y 2005 *Phys. Rev. B* **72** 045356
[42] Hamaya K, Masubuchi S, Kawamura M, Machida T, Jung M, Shibata K, Hirakawa K, Taniyama T, Ishida S and Arakawa Y 2007 *Appl. Phys. Lett* **90** 053108
[43] Zhang Y T, Guo Y and Li Y C 2005 *Phys. Rev. B* **72** 125334
[44] Lv H F and Guo Y 2008 *Appl. Phys. Lett.* **92** 062109
[45] Press D, Ladd T D, Zhang B Y and Yamamoto Y 2008 *Nature* **456** 218.
[46] Ying Y B and Jin G J 2010 *Appl. Phys. Lett.* **96** 093104
[47] Frolov S M, Venkatesan A, Yu W, Folk J A and Wegscheider W 2009 *Phys. Rev. Lett.* **102** 116802
[48] Frolov S M, Lüscher S, Yu W, Ren Y, Folk J A and Wegscheider W 2009 *Nature* **458** 868
[49] Chi F and Sun Q F 2010 *Phys. Rev. B* **81** 075310
[50] Sun Q F, Guo H and Wang J 2003 *Phys. Rev. Lett.* **90** 258301
[51] Long W, Sun Q F, Guo H and Wang J 2003 *Appl. Phys. Lett.* **83** 1397
[52] Wang D K, Sun Q F and Guo H 2004 *Phys. Rev. B* **69** 205312
[53] Chen Z Z, Lü R and Zhu B F 2005 *Phys. Rev. B* **71** 165324
[54] Wang R Q, Zhou Y Q, Wang B G and Xing D Y 2007 *Phys. Rev. B* **75** 045318
[55] Liu Y S, Chen H, Fan X H and Yang X F 2006 *Phys. Rev. B* **73** 115310